Research Article

Structural, Spectroscopic Investigation and Quantum Chemical Calculation Studies of 2,4,6-trimethylphenol for Pharmaceutical Application

S. Jeyavijayan[1]*, E. Gobinath[1], J. Senthil Kumar[2]
1Department of Physics, Kalasalingam University, Anand Nagar, Krishnankoil 626 126, Tamil Nadu, India.
2PG & Research Department of Physics, Periyar EVR College, Tiruchirappalli 620 023, India.
***Corresponding author's E-mail:** sjeyavijayan@gmail.com

Accepted on: 10-08-2016; **Finalized on:** 31-10-2016.

ABSTRACT

The FTIR and FT-Raman spectra of 2,4,6-trimethylphenol (TMP) have been recorded in the regions 4000-400 cm^{-1} and 3500-50 cm^{-1}, respectively. The optimum molecular geometry, harmonic vibrational frequencies, infrared intensities and Raman scattering activities were calculated by *ab initio* Hartree–Fock (HF) and density functional theory (DFT/B3LYP) methods using 6-31+G(d,p) basis set. The normal modes are assigned with the help of total energy distribution (TED) analysis. The observed vibrational wavenumbers were compared with the calculated results. The difference between the observed and scaled wavenumber values of most of the fundamentals is very small. The calculated first hyperpolarizability results show that TMP may have microscopic nonlinear optical (NLO) behavior with non-zero values. The effects of frontier orbitals, HOMO and LUMO, transition of electron density transfer have been discussed. Besides, molecular electrostatic potential (MEP), Mulliken's charges analysis, and several thermodynamic properties were performed.

Keywords: FTIR, FT-Raman, 2,4,6-trimethylphenol , DFT calculations, MEP.

INTRODUCTION

Phenol and its derivatives are interesting molecules for theoretical studies due to their relatively small size and similarity to biological species. They are also the versatile precursor to a large collection of drugs, most notably aspirin but also many herbicides and pharmaceuticals. Phenol derivatives are used in the preparation of cosmetics including sunscreens, hair dyes and skin lightening preparations. Unlike normal alcohols, phenols are acidic because of the influence of the aromatic ring[1]. Phenol and its vapours are corrosive to the eyes, the skin and the respiratory tract. In recent years, phenol and substituted phenol have been the frequent subjects of experimental and theoretical work because of their significance in industry and environment. Evans[2] has extensively studied the vibrational assignments of infrared spectrum of phenol. The DFT studies on the phenol and thiophenol interaction on an undecagold cluster surface have been investigated by Jayanthi *et al*[3]. Jianhan Huang *et al.*[4] have elucidated halogen effect and isotope effect of Chloro Phenol and Gui-xiangWang *et al*.[5] have obtained the vibrational analysis on nitro phenols. The vibrational spectroscopy investigation using *ab initio* (HF) and DFT (B3LYP) calculations on the structure of 3-Bromo phenol have been studied by Mahadevan *et al*[6]. From the spectroscopic point of view, in recent years numerous experimental and theoretical studies have been made on the vibrational spectra of phenol derivatives[7-9]. More recently, the FT-IR and DFT study of the free and solvated 4-(imidazol-1-yl) phenol have been studied by Yurdakul *et al*[10].

During the course of investigation on the samples of biological and pharmaceutical active compounds, our attention has been turned towards 2,4,6-trimethylphenol (TMP). It is one of the most important organic intermediates, are widely used for the manufacture of pesticides, rubber, drugs, varnishes and dyestuffs. The assignment of the vibrational frequencies for substituted phenols becomes complicated problem because of the superposition of several vibrations due to fundamentals and due to substituents. However, a comparison of the spectra with that of the parent compound gives some definite clues about the nature of the molecular vibrations.

Literature survey reveals that to the best of the knowledge, no *ab initio*/DFT frequency calculations for 2,4,6-trimethylphenol have been reported so far for the frequency assignments. Therefore, the present investigation was undertaken to study the vibrational spectra of the molecule completely and to identify the various normal modes with greater wave numbers accurately. In this study, *ab initio* HF and density functional theory (DFT) calculations have been performed to support our wave number assignments.

MATERIALS AND METHODS

The pure sample of TMP obtained from Lancaster chemical company, UK and used as such for the spectral measurements. The room temperature Fourier transform infrared spectra of the title compound was recorded in the region 4000-400 cm^{-1}, at a resolution of $\pm$ 1 cm^{-1} using BRUKER IFS 66V model FTIR spectrometer equipped with an MCT detector, a KBr beam splitter and globar source.

The FT-Raman spectrum of TMP was recorded on a computer interfaced BRUKER IFS 66V model interferometer equipped with FRA-106 FT-Raman accessories. The spectrum was measured in the Stokes region 3500-50 cm^{-1} using Nd: YAG laser operating at 200 mW power continuously with 1064nm excitation. The reported wave numbers are expected to be accurate within $\pm$1 cm^{-1}.

Computational Details

In order to provide information with regard to the structural characteristics and the normal vibrational modes of TMP, the *ab initio* HF and DFT-B3LYP correlation functional calculations have been carried out. The molecular geometry optimizations, energy and vibrational frequency calculations were carried out for TMP with the GAUSSIAN 09W software package[11]. Initial geometry generated from the standard geometrical parameters was minimized without any constraint on the potential energy surface at HF level adopting the standard 6-31+G(d,p) basis set. This geometry was then re-optimized again at DFT level employing the Becke 3LYP keyword, which invokes Becke's three-parameter hybrid method[12] using the correlation function of Lee *et al.*[13], implemented with the same basis set. The optimized structural parameters were used for the vibrational frequency calculations at DFT level to characterize all the stationary points as minima. The multiple scaling of the force constants were performed according to SQM procedure[14] using selective scaling in the natural internal coordinate representation. The transformation of force field and calculation of the TED were done on a PC with the MOLVIB program (version V7.0-G77) written by Sundius[15,16]. By the use of GAUSSVIEW molecular visualization program[17] along with available related molecules, the vibrational frequency assignments were made by their TED with a high degree of confidence. The TED elements provide a measure of each internal coordinate's contributions to the normal coordinate.

RESULTS AND DISCUSSION

Molecular geometry

The optimized molecular structure of TMP is shown in Fig. 1. The global minimum energy obtained by the HF and DFT structure optimization using 6-31+G(d,p) basis set for TMP are calculated as -422.70193282 and -425.45596685 Hartrees, respectively. The optimization geometrical parameters of TMP obtained by the HF and DFT/B3LYP methods with 6-31+G(d,p) basis set are listed in the Table 1. From the structural data given in Table 1, it is observed that the geometrical parameters are found to be almost same at HF/6-31+G(d,p) and B3LYP/6-31+G(d,p) levels. However, the B3LYP/6-31+G(d,p) level of theory, in general slightly over estimates bond lengths but it yields bond angles in excellent agreement with the HF method. The calculated geometrical parameters are the bases for calculating other parameters such as vibrational frequencies and thermodynamics properties of the compound. According to the calculation (B3LYP/6-31+(d, p)), the order of the bond length is C5-C6 < C3-C4 < C2-C3 = C4-C5 < C1-C2 < C1-C6. From the order of the bond length, it is clear that the hexagonal structure of the benzene ring slightly distorted. This can be due to the influence of conjugation between the substituents and the ring. Normally the O-H group oxygen from its strong electron-withdrawing nature in the para position is expected to increase the contribution of the resonance structure. This is evidenced by the larger C–O bond length calculated by B3LYP/6-31+(d, p) method is 1.3789 Å. The ring carbon atoms in substituted benzenes exerts a larger attraction on the valence electron cloud of the hydrogen atom resulting in an increase in the C-H force constants and a decrease in the corresponding bond length. It is evident from the C–H bond lengths in TMP vary from 1.0881 to 1.0884Å by B3LYP/6-31+(d,p) method. The benzene ring appears to be a little distorted because of the O-H group and methyl group substitutions as seen from the bond angles C2–C1–C6, C1–C6–C5, C5–C4–C3 and C3–C2–C1, which are calculated as 121.69°, 117.95°, 117.77° and 118.09°, respectively, by B3LYP/6-31+(d,p) method and are differ from their typical hexagonal angle of 120°.

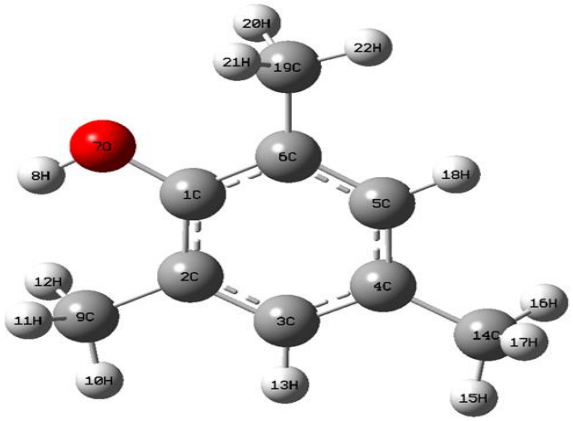

Figure 1: Molecular structure of 2,4,6-trimethylphenol

Vibrational assignments

From the structural point of view the molecule is assumed to have C_1 point group symmetry and hence, all the calculated frequency transforming to the same symmetry species (A). The molecule consists of 22 atoms and expected to have 60 normal modes of vibrations. All the vibrations are active both in the Raman scattering and infrared absorption. The detailed vibrational assignment of fundamental modes of TMP along with the calculated IR and Raman frequencies, IR intensity, Raman activity and normal mode descriptions (characterized by TED) are reported in Table 2. The observed FTIR and FT-Raman spectra of TMP are shown in Figs. 2.

The main focus of the present investigation is the proper assignment of the experimental frequencies to the various vibrational modes of TMP in corroboration with the calculated harmonic vibrational frequencies at HF and

B3LYP levels using the standard 6-31+G(d,p) basis set. Comparison of the frequencies calculated by HF and DFT-B3LYP methods with the experimental values reveals the overestimation of the calculated vibrational modes due to neglect of anharmonicity in real system.

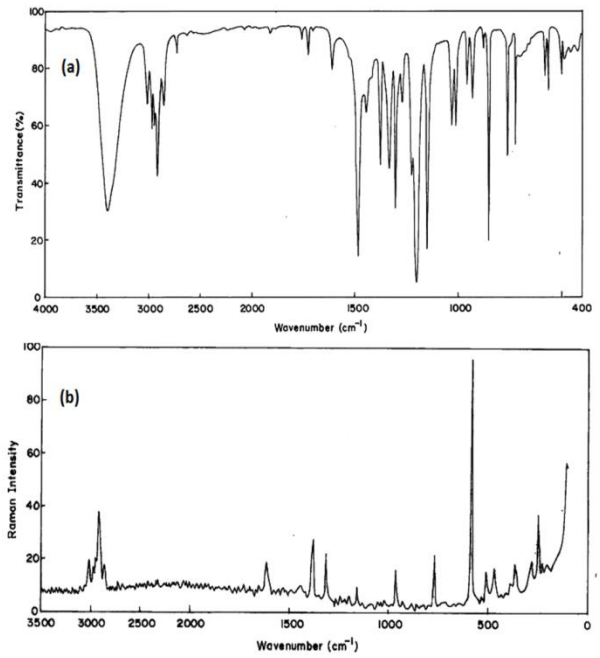

Figure 2: (a) FTIR and (b) FT-Raman spectrum of 2,4,6-trimethylphenol.

The results indicate that the B3LYP/6-31+G(d,p) calculations approximate the observed fundamental frequencies much better than the HF/6-31+G(d,p) results. The vibrational analysis obtained for TMP with the unscaled HF and B3LYP force field is generally somewhat greater than the experimental values. These discrepancies can be corrected either by computing anharmonic corrections explicitly or by introducing a scaled field or directly scaling the calculated wavenumbers with proper factor[6]. A tentative assignment is often made on the basis of the unscaled frequencies by assuming the observed frequencies so that they are in the same order as the calculated ones. Then, for an easier comparison to the observed values, the calculated frequencies are scaled by the scale to less than 1, to minimize the overall deviation. A better agreement between the computed and experimental frequencies can be obtained by using different scale factors for different regions of vibrations For that purpose, a scaling factor of 0.90 (above 1800 cm^{-1}) and 0.92 (below 1800 cm^{-1}) for the fundamental modes except the torsional mode has been utilised to obtain the scaled frequencies of the compound TMP in HF level. Similarly, a scale factor of 0.925 (up to 1700 cm^{-1}) and 0.97 (below 1700cm^{-1}) was used to compute the corrected wavenumbers at DFT level and compared with the experimentally observed frequencies. The resultant scaled frequencies are also listed in Table 2.

O-H vibrations

Bands due to O-H stretching are of medium to strong intensity in the infrared spectrum, although it may be broad. In Raman spectra the band is generally weak. In phenols, the free O-H group absorbs at 3615 cm^{-1} while the associated group has a stretching frequency in the range 3145-3430 cm^{-1}. This is due to the intermolecular hydrogen bonding[18]. The O-H stretching bands move to lower frequencies usually with increased intensity and band broadening in the hydrogen bonded species. In TMP, the FTIR band appeared at 3396 cm^{-1} is assigned to O-H stretching modes of vibration, which is further supported by the TED contribution of 99%. The O-H in-plane-bending vibration in phenol, in general, lies in the region 1150-1250 cm^{-1} and is not much affected due to hydrogen bonding unlike the stretching and out-of-plane deformation frequencies. The O-H out-of-plane deformation vibration in phenols lies in the region 290-320 cm^{-1} for free O-H and in the region 517-710 cm^{-1} for associated O-H[19]. Hence, in this study, the in-plane and out-of-plane bending vibrations of hydroxy group have been identified at 1256 and 385 cm^{-1} in the FT-Raman for TMP, respectively. These bending modes show consistent agreement with the computed B3LYP results.

C-H vibrations

Aromatic compounds commonly exhibit multiple weak bands in the region 3100-3000 cm^{-1} due to aromatic C-H stretching vibrations[20]. Hence, the Raman bands appeared at 3180 and 3100 cm^{-1} in TMP have been assigned to C-H stretching vibrations and these modes are confirmed by their TED values. The bands due to C-H in-plane ring bending vibrations, interact somewhat with C-C stretching vibrations, are observed as a number of sharp bands in the region 1300-1000 cm^{-1}. The C-H out-of-plane bending vibrations are strongly coupled vibrations and occur in the region 900-667 cm^{-1}. The FT-Raman bands at 1226, 1202 cm^{-1} and infrared band at 1230 cm^{-1} are assigned to C–H in-plane bending vibrations of TMP. The out-of-plane bending vibrations of C-H group have also been identified for TMP and they were presented in Table 2. The theoretically computed values for C-H vibrational modes by B3LYP/6-31+G(d,p) method gives excellent agreement with experimental data.

CH_3 group vibrations

For the assignments of CH_3 group frequencies one can expect nine fundamentals to be associated with each CH_3 group, namely the symmetrical stretching in CH_3 (CH_3 sym. stretching); asymmetrical stretching (i.e. in-plane hydrogen stretching mode); the symmetrical (CH_3 sym. deformation) and asymmetrical (CH_3 asy. deformation) deformation modes; the in-plane rocking (CH_3 ipr), out-of-plane rocking (CH_3 opr) and twisting t(CH_3) modes.

Table 1: Optimized geometrical parameters of 2,4,6-trimethyl phenol obtained by HF and B3LYP using 6-31+G(d,p) basis set calculations

Parameter Bond length	Value (Å)		Bond angle	Value (°)		Dihedral Angle	Value (°)	
	HF	B3LYP		HF	B3LYP		HF	B3LYP
C1-C2	1.3869	1.4030	C2-C1-C6	121.5268	121.6991	C6-C1-C2-C3	0.0009	0.1062
C1-C6	1.3955	1.4051	C2-C1-O7	122.1702	122.0006	C6-C1-C2-C9	180.0016	-179.7411
C1-O7	1.3609	1.3789	C6-C1-O7	116.303	116.3	O7-C1-C2-C3	-180.0029	179.8806
C2-C3	1.3947	1.4020	C1-C2-C3	118.2457	118.0958	O7-C1-C2-C9	-0.0021	0.0333
C2-C9	1.5123	1.5117	C1-C2-C9	120.9394	120.7048	C2-C1-C6-C5	-0.0014	-0.1187
C3-C4	1.3834	1.3975	C3-C2-C9	120.8148	121.1992	C2-C1-C6-C19	-180.0022	179.7318
C3-H13	1.077	1.0881	C2-C3-C4	122.0622	122.1348	O7-C1-C6-C5	180.0021	-179.9053
C4-C5	1.3938	1.4020	C2-C3-H13	118.5066	118.4884	O7-C1-C6-C19	0.0013	-0.0547
C4-C14	1.5119	1.5124	C4-C3-H13	119.4312	119.3767	C2-C1-O7-H8	-0.0216	0.13
C5-C6	1.3839	1.3971	C3-C4-C5	117.7929	117.7787	C6-C1-O7-H8	-180.0251	179.9159
C5-H18	1.0776	1.0884	C3-C4-C14	121.6025	121.3149	C1-C2-C3-C4	-0.0003	0.07
C6-C19	1.5088	1.5081	C5-C4-C14	120.6045	120.9003	C1-C2-C3-H13	-179.9991	-179.8671
O7-H8	0.9414	0.9651	C4-C5-C6	122.2087	122.3329	C9-C2-C3-C4	-180.0011	179.9165
C9-H10	1.0827	1.0929	C4-C5-H18	119.1943	119.2766	C9-C2-C3-H13	0.0002	-0.0206
C9-H11	1.0883	1.0991	C6-C5-H18	118.597	118.3904	C1-C2-C9-H10	-180.0059	179.9556
C9-H12	1.0883	1.0991	C1-C6-C5	118.1636	117.9582	C1-C2-C9-H11	-60.6126	-60.6986
C14-H15	1.0842	1.0943	C1-C6-C19	119.942	120.038	C1-C2-C9-H12	60.6022	60.5844
C14-H16	1.0862	1.0957	C5-C6-C19	121.8944	122.0036	C3-C2-C9-H10	-0.0052	0.1131
C14-H17	1.0862	1.0974	C1-O7-H8	111.9087	110.1003	C3-C2-C9-H11	119.3882	119.4588
C19-H20	1.0851	1.0959	C2-C9-H10	110.6111	110.6784	C3-C2-C9-H12	-119.397	-119.2581
C19-H21	1.0851	1.0935	C2-C9-H11	111.8566	112.1986	C2-C3-C4-C5	0.0003	-0.2227
C19-H22	1.0838	1.0959	C2-C9-H12	111.8562	112.2138	C2-C3-C4-C14	179.9884	178.8852
			H10-C9-H11	107.1763	106.9241	H13-C3-C4-C5	179.9991	179.7138
			H10-C9-H12	107.1753	106.9363	H13-C3-C4-C14	-0.0128	-1.1783
			H11-C9-H12	107.9284	107.5931	C3-C4-C5-C6	-0.0009	0.2096
			C4-C14-H15	111.1311	111.3101	C3-C4-C5-H18	-179.9977	-179.7047
			C4-C14-H16	111.2298	111.502	C14-C4-C5-C6	-179.9891	-178.9021
			C4-C14-H17	111.2271	111.4485	C14-C4-C5-H18	0.014	1.1835
			H15-C14-H16	107.7668	107.7644	C3-C4-C14-H15	0.077	14.9116
			H15-C14-H17	107.7653	107.4376	C3-C4-C14-H16	120.1498	135.2873
			H16-C14-H17	107.5462	107.1594	C3-C4-C14-H17	-119.992	-105.0122
			C6-C19-H20	111.0719	111.3007	C5-C4-C14-H15	-179.9352	-166.0083
			C6-C19-H21	111.0707	110.7735	C5-C4-C14-H16	-59.8624	-45.6325
			C6-C19-H22	110.5733	111.3073	C5-C4-C14-H17	59.9958	74.0679
			H20-C19-H21	107.0805	108.3905	C4-C5-C6-C1	0.0014	-0.0439
			H20-C19-H22	108.4613	106.5111	C4-C5-C6-C19	180.0023	-179.8913
			H21-C19-H22	108.4589	108.3954	H18-C5-C6-C1	179.9983	179.8712
						H18-C5-C6-C19	-0.0009	0.0238
						C1-C6-C19-H20	-59.5179	59.3912
						C1-C6-C19-H21	59.5449	-179.9402
						C1-C6-C19-H22	-179.9884	-59.261
						C5-C6-C19-H20	120.4813	-120.7645
						C5-C6-C19-H21	-120.456	-0.0959
						C5-C6-C19-H22	0.0107	120.5833

For numbering of atoms refer Fig.1.

Table 2: The observed FTIR, FT-Raman and calculated (Unscaled and Scaled) frequencies (cm^{-1}), IR intensity (Km mol^{-1}), Raman Activity ($Å^4$ amu^{-1}) and probable assignments (characterized by TED) of 2,4,6- trimethyl phenol using HF/6-31+G(d,p) and B3LYP/6-31+G(d,p) calculations

Sl. No.	Species	Observed fundamentals (cm^{-1})		Calculated frequencies ν_i (cm^{-1})								TED(%) among types of internal coordinates
				HF/6-31+G(d,p)				B3LYP/6-31+G(d,p)				
		FTIR	Raman	Unscaled ν_i	Scaled	IR intensity	Raman activity	Unscaled ν_i	Scaled	IR intensity	Raman activity	
1	A	3396 (s)	-	4219	3797	94.5646	60.9359	3843	3554	59.1577	82.4816	νOH (99)
2	A	-	3180 (w)	3335	3001	19.7147	98.0702	3165	2927	11.4069	141.4477	νCH (98)
3	A	-	3100 (s)	3329	2996	25.3010	80.0126	3163	2925	29.5056	64.2694	νCH (96)
4	A	-	3019 (w)	3269	2942	18.3736	56.5309	3122	2887	13.7496	61.2399	CH_3ss (92)
5	A	3013 (w)	-	3264	2937	26.0454	63.5454	3121	2886	16.3158	62.8403	CH_3ss (94)
6	A	-	2980 (w)	3255	2929	26.3565	62.4871	3111	2877	18.3483	63.7400	CH_3ss (91)
7	A	2973(ms)	-	3247	2922	23.4498	82.4407	3091	2859	15.9941	91.8800	CH_3ips (90)
8	A	2944 (w)	-	3230	2907	28.4780	83.9146	3083	2851	20.6421	94.3425	CH_3ips (89)
9	A	2917 (w)	2918 (w)	3206	2885	30.9746	85.3562	3053	2824	22.1331	96.6577	CH_3ips (88)
10	A	2857(ms)	-	3189	2870	41.4264	191.3184	3038	2810	34.2210	248.1896	CH_3 ops (90)
11	A	-	2850 (w)	3178	2860	51.1588	178.9046	3029	2801	47.7913	243.7076	CH_3ops (91)
12	A	-	2740 (w)	3161	2844	49.0219	170.9271	3008	2782	44.1165	223.9733	CH_3 ops (87)
13	A	1740 (s)	-	1807	1626	0.0079	15.4485	1658	1608	0.1009	20.9929	νCC (86)
14	A	1728(vw)	-	1800	1620	5.9648	15.5750	1650	1600	3.5568	18.7926	νCC (87)
15	A	-	1720 (w)	1657	1524	103.7226	4.5233	1530	1484	83.3311	3.9679	νCC (85)
16	A	-	1640 (vw)	1632	1501	19.9148	9.1012	1513	1467	23.1319	8.3127	νCC (84)
17	A	1612 (s)	-	1620	1490	5.9386	0.7822	1500	1455	2.3411	1.5284	νCC (82)
18	A	-	1604 (vw)	1614	1484	6.8782	11.9531	1496	1451	7.887	10.6158	νCC (83)
19	A	-	1495 (w)	1608	1479	4.2031	10.7561	1491	1446	5.2912	9.8333	νCC (85)
20	A	1488(ms)	-	1603	1474	6.7119	9.1792	1483	1438	8.0047	8.0505	νCC (80)
21	A	1446(ms)	-	1597	1469	25.2877	7.3726	1473	1428	27.0126	27.0126	νCC (82)
22	A	-	1440 (w)	1570	1444	1.8993	3.1032	1451	1407	2.5180	5.8053	CH_3 ipb (80)
23	A	1376 (w)	-	1551	1426	0.8973	9.2295	1423	1380	0.8919	22.5779	CH_3 ipb (81)
24	A	-	1365 (s)	1546	1422	1.117	7.2059	1420	1377	1.4731	19.4246	CH_3 ipb (78)
25	A	1338 (vs)	-	1544	1420	0.1368	5.2721	1419	1376	0.4509	10.9122	CH_3 sb (79)
26	A	1306 (s)	-	1433	1318	2.0251	8.8316	1363	1322	18.7650	1.6813	CH_3 sb (76)
27	A	-	1300 (s)	1425	1311	66.1678	3.7685	1338	1297	6.2135	23.5772	CH_3 sb (75)
28	A	1272 (s)	-	1367	1257	71.3789	4.6711	1296	1257	16.8657	1.5262	νCO (74)
29	A	-	1256 (vw)	1338	1230	60.6588	2.7134	1260	1222	48.7272	1.7297	bOH (72)
30	A	1226(ms)	1230 (w)	1280	1177	36.7928	2.7517	1215	1178	129.7939	3.7042	bCH (71)
31	A	1202(ms)	-	1263	1161	38.6501	6.2146	1176	1140	32.1744	6.3985	b CH (70)
32	A	-	1196 (w)	1164	1070	2.9144	0.1003	1062	1030	0.3946	0.1192	CH_3 opb (72)
33	A	1160(ms)	-	1161	1068	0.3697	0.4058	1061	1029	4.0698	1.6840	CH_3 opb (68)
34	A	-	1150 (vw)	1153	1060	0.1336	0.5953	1056	1024	2.5354	0.2580	CH_3 opb (71)
35	A	1031(ms)	-	1118	1028	8.8292	2.2987	1041	1009	18.8843	0.7846	Rtrigd (69)
36	A	1012 (w)	1010 (w)	1111	1022	12.6543	1.5019	1033	1002	1.2307	2.1304	Rsymd (68)
37	A	969 (w)	-	1082	995	16.3291	0.2363	1024	993	10.9027	0.4325	Rasymd (67)
38	A	-	958 (ms)	1038	954	0.9292	11.6543	972	942	6.6623	12.8851	CH_3 opr (66)
39	A	932 (ms)	-	1010	929	0.4895	0.3588	937	908	7.2656	0.0912	CH_3 opr (69)
40	A	-	920 (w)	1002	921	7.2172	0.6959	895	868	0.7823	0.5820	CH_3 opr (68)
41	A	-	880 (vw)	974	896	30.2844	0.2025	867	840	21.9720	0.2324	CH_3 ipr (69)
42	A	853 (vs)	-	828	761	11.0892	7.9539	772	748	11.9575	8.0693	CH_3 ipr (66)
43	A	762 (s)	765 (s)	811	746	6.2519	0.3464	725	703	3.2274	0.3194	CH_3 ipr (65)
44	A	723 (s)	-	635	584	2.8140	0.0583	583	565	5.7534	4.7181	b CC (65)
45	A	711 (ms)	-	627	576	6.4734	4.8127	581	563	2.0944	2.2541	b CC (64)
46	A	706 (ms)	-	608	559	0.0670	27.5733	575	557	0.3225	21.8820	b CC (66)
47	A	701 (w)	-	556	511	0.0005	0.2798	506	490	1.5654	0.6987	b CO (65)
48	A	682 (ms)	-	542	498	3.3078	1.8179	504	488	1.2418	0.6646	ω CH (61)
49	A	-	578 (s)	495	455	2.3854	6.5875	463	449	2.0786	6.2511	ω CH (62)
50	A	565 (w)	-	392	360	0.1399	1.5869	356	345	0.1790	1.1791	t Rtrigd (60)
51	A	-	520 (vw)	354	325	4.4151	0.0772	327	317	4.2889	0.0645	t Rsymd (61)
52	A	501 (w)	501 (w)	300	276	1.2175	0.4527	291	282	84.0559	0.8050	t R asymd (60)
53	A	493 (w)	-	289	265	0.7327	0.4738	279	270	1.1223	0.7033	ω CC (58)
54	A	482 (vw)	-	265	243	21.5225	1.1967	270	261	0.8721	0.7620	ω CC (59)
55	A	457 (vw)	460 (w)	203	186	81.1367	1.6465	227	220	12.0682	2.8984	ω CC (60)
56	A	426 (vw)	-	187	172	7.5536	0.3690	177	171	4.1993	0.0742	ω CO (61)
57	A	-	385 (ms)	168	154	6.2440	0.1587	152	147	0.3022	0.0478	ω OH (58)
58	A	-	350 (vw)	146	134	1.6362	0.3496	130	126	0.0088	0.2160	CH_3 twist (57)
59	A	-	277 (w)	131	120	1.6830	0.1357	121	117	0.0114	0.1234	CH_3 twist (56)
60	A	-	251 (w)	36	33	1.933	0.1738	42	40	0.2795	0.3889	CH_3 twist (57)

Abbreviations: *w-weak, s-strong. ms-medium strong, vw-very weak, vs-very strong, R-ring, b-bending, v-streching, symd-symmetric deformation, ω-out-of-plane bending, asymd-antisymmetric deformation, trigd-trigonal deformation, ss-symmetric streching, ips-in-plane stretching, sb-symmetric bending, ipb-in-plane-bending, ipr-in-plane-rocking, ops-out-of-plane stretching, opb-out-of-plane bending, opr-out-of-planerocking,t-torsion.*

Table 3: Thermodynamic properties of 2,4,6-trimethylphenol.

Parameters	Method/Basis set	
	HF/6-31+G(d,p)	B3LYP/6-31+G(d,p)
Optimized global minimum Energy (Hartrees)	-422.7019	-425.4559
Total energy(thermal), E_{total} (kcal mol^{-1})	131.644	124.074
Heat capacity, C_v (cal mol^{-1} k^{-1})	37.645	40.051
Entropy, S (cal mol^{-1} k^{-1})		
Total	99.135	100.731
Translational	40.637	40.637
Rotational	29.647	29.684
Vibrational	28.852	30.410
Vibrational energy, E_{vib} (kcal mol^{-1})	129.866	122.296
Zero point vibrational energy, (kcal mol^{-1})	125.16194	117.28832
Rotational constants (GHz)		
A	1.75750	1.73766
B	1.26882	1.25180
C	0.74697	0.73763
Dipole moment (Debye)		
μ_x	0.1232	-0.0035
μ_y	-1.4491	-1.4137
μ_z	-0.0004	0.0256
μ_{total}	1.4544	1.4140

In addition to that, CH_3 ops, out-of-plane stretch, and CH_3 opb, out-of-plane bending modes of the CH_3 group would be expected to be depolarized for asymmetry species. The C-H stretching in CH_3 occurs at lower frequencies than those of the aromatic ring (3100-3000cm^{-1}). The vibrations of the methyl group in the TMP are observed in the typical range reported earlier[21]. The asymmetric and symmetric stretching vibrations are observed in the ranges 3010-2970 and 2940-2900 cm^{-1}. In the present study, the CH_3 symmetric and in-plane stretching frequencies are established at 3013, 2973, 2944, 2917 and 3019, 2980, 2918 cm^{-1} in FTIR and Raman spectrum, respectively. We have observed the CH_3 in-plane bending modes of TMP at 1440, 1376, 1365 cm^{-1} and CH_3 symmetric bending modes at 1338, 1306, 1300 cm^{-1} in infrared and Raman spectra. The CH_3 deformation modes mainly coupled with in-plane bending vibrations. The bands obtained at 762, 853, 932 cm^{-1} in IR and 765, 880, 920, 958 cm^{-1} in Raman are assigned to CH_3 in-plane and out-of-plane rocking modes. The CH_3 out-of-plane stretching and out-of-plane bending modes are found at 2857, 2850, 2740 cm^{-1} and 1196, 1160, 1150 cm^{-1} in the experimental spectra, respectively. The assignment of band at 350, 277, 251 cm^{-1} in the FT-Raman is attributed to CH_3 twisting modes. These assignments are substantiated by the reported literature[22].

C–C vibrations

The C-C aromatic stretching vibrations gives rise to characteristic bands in both the observed IR and Raman spectra, covering the spectral range[23] from 1625 to 1400 cm^{-1}. Therefore, the C-C stretching vibrations of the title compound are found at 1740, 1728, 1612, 1488, 1446 cm^{-1} in FTIR and 1720, 1640, 1604, 1495 cm^{-1} in the FT-Raman spectrum and these modes are confirmed by their TED values. Most of the ring vibrational modes are affected by the substitutions in the aromatic ring of TMP. In the present study, the bands observed at 1031, 1012, 969 cm^{-1} and 1010 cm^{-1} in the FTIR and Raman spectrum, respectively, have been designated to ring in-plane bending modes by careful consideration of their quantitative descriptions. The ring out-of-plane bending modes of TMP are also listed in the Table 2. The reductions in the frequencies of these modes are due to the change in force constant and the vibrations of the functional groups present in the molecule.

C-O vibrations

The interaction of carbonyl group with other groups present in the system did not produce such a drastic and characteristics changes in the frequency of C-O stretch as did by the interaction of O-H stretch. In this present work, a strong IR band is observed at 1272 cm^{-1} due to the stretching vibration between carbon and oxygen atoms which is in line with the literature[24]. The IR band appeared at 701 cm^{-1} in TMP has been designated to C-N in-plane bending vibration. The C-N out-of-plane bending vibration observed at 426 cm^{-1} in IR spectrum. These assignments are also supported by the TED values.

First hyperpolarizability

The quantum chemistry based prediction of non-linear optical (NLO) properties of a molecule has an important role for the design of materials in modern communication technology, signal processing and optical interconnections[25]. Especially organic molecules are studied because of their larger NLO susceptibilities arising π-electron cloud movement from donor to acceptor, fast

NLO response times, high laser damage thresholds and low dielectric constants. Although the organic molecules have these advantages, they have several NLO disadvantages, too: they have generally low thermal stability and they may undergo a facile relaxation to random orientation[26]. In addition, in the UV–vis region, the low energy transitions result in a trade-off between the nonlinear efficiency and optical transparency[27]. But the usage of organic molecules as ligands can overcome these disadvantages. The total static dipole moment μ, the average linear polarizability $\overline{\alpha}$, the anisotropy of the polarizability $\Delta\alpha$, and the first hyperpolarizability β can be calculated by using the following Equations[25]:

The calculated values of total static dipole moment μ, the average linear polarizability $\overline{\alpha}$, the anisotropy of the polarizability $\Delta\alpha$, and the first hyperpolarizability β using the DFT-B3LYP/6-31+G(d,p) method are 1.414 Debye, 16.307Å^3, 1.3264Å^3 and 2.8065×10^{-30} e.s.u.$^{-1}$, respectively. The values of μ, $\overline{\alpha}$ and β obtained by Sun *et al*.[28] with the B3LYP method for urea are 1.373 Debye, 3.831 Å^3 and 0.3729×10^{-30} e.s.u.$^{-1}$, respectively. The first hyperpolarizability of TMP molecule is 7.5 times greater than that of urea. According to these results, the title compound may be a potential applicant in the development of NLO materials.

HOMO, LUMO analysis

The highest occupied molecular orbitals (HOMOs) and the lowest- lying unoccupied molecular orbitals (LUMOs) are named as frontier molecular orbitals (FMOs). The FMOs play an important role in the electric and optical properties, as well as in UV–Vis spectra and chemical reactions[29]. The atomic orbital HOMO and LUMO compositions of the frontier molecular orbital for TMP computed at the B3LYP/6-31+G(d,p) are shown in Fig. 3, which reveals that the energy gap reflects the chemical activity of the molecule.

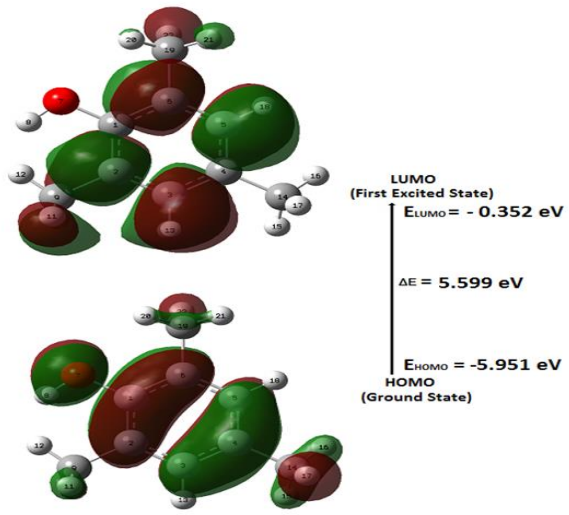

Figure 3: The atomic orbital HOMO and LUMO compositions of the frontier molecular orbital for 2,4,6-trimethylphenol

The calculations indicate that the title compound have 37 occupied MOs. The LUMO: of π nature, (i.e. benzene ring) is delocalized over the whole C-C bond. By contrast, the HOMO is located over OH group; consequently the HOMO → LUMO transition implies an electron density transfer to C-C bond of the benzene ring and methyl groups from OH group. Moreover, these three orbitals significantly overlap in their position of the benzene ring for TMP. The LUMO as an electron acceptor represents the ability to obtain an electron, and HOMO represents the ability to donate an electron. Moreover, a lower HOMO–LUMO energy gap explains the fact that eventual charge transfer interaction is taking place within the molecule.

Mulliken Population Analysis

The charge distribution on the molecule has an important influence on the vibrational spectra. The total atomic charges of TMP obtained by Mulliken[30] using HF and B3LYP methods with 6-31+G(d,p) basis set are represented in graphical form as shown in Fig. 4 and it gives us information about the charge shifts relative to TMP. More charge density was found at C2, C4 and C6 than that of other ring carbon atoms. The high positive charge at C2, C4 and C6 is due to the effect of electron releasing methyl group attached with these atoms. The electron donating character of the hydroxyl group in the title compound is demonstrated by a decrease of electron density on C1 atom. From the result it is clear that the substitution of hydroxyl and methyl groups in the aromatic ring leads to a redistribution of electron density.

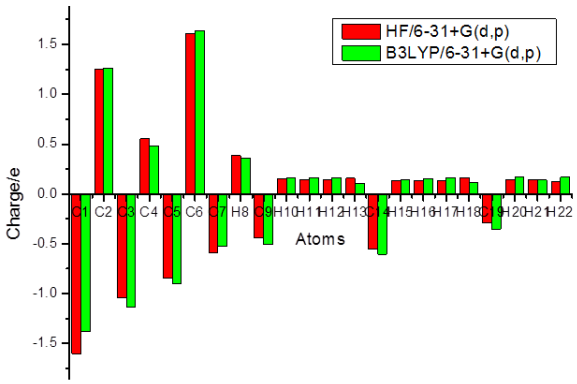

Figure 4: Mulliken's plot for 2,4,6-trimethylphenol

Molecular electrostatic potential (MEP)

MEP is related to the electron density and is a very useful descriptor in understanding sites for electrophilic and nucleophilic reactions as well as hydrogen bonding interactions[31]. The electrostatic potential is also well suited for analyzing processes based on the ''recognition'' of one molecule by another, as in drug-receptor, and enzyme-substrate interactions, because it is through their potentials that the two species first ''see'' each other[32]. To predict reactive sites of electrophilic and nucleophilic attacks for the investigated molecule, MEP at the B3LYP optimized geometry was calculated as shown in Fig. 5.

The different values of the electrostatic potential represented by different colors; red represents the regions of the most negative electrostatic potential, blue represents the regions of the most positive electrostatic potential and green represents the region of zero potential. The color code of these maps is in the range between -0.05393 (deepest red) and +0.05393 (blue) in the title compound, where blue indicates the strongest attraction and red indicates the strongest repulsion. The negative (red and yellow) regions of MEP were related to electrophilic reactivity and the positive (blue) regions to nucleophilic reactivity. From the MEP diagram, it is evident that the negative charge covers the oxygen atom of hydroxyl group and the positive region is over the hydrogen atom of methyl groups. The more electro negativity in the oxygen atom of O-H group makes it the most reactive part in the molecule.

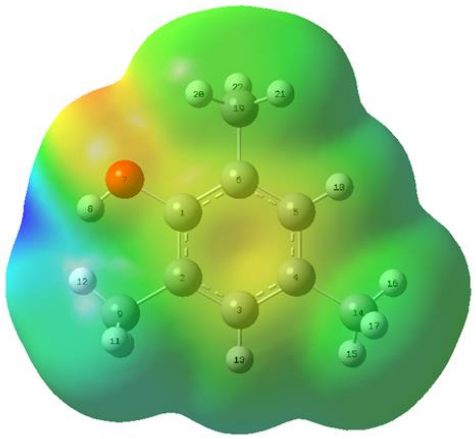

Figure 5: MEP map for 2,4,6-trimethylphenol.

Other molecular properties

Normally, the thermo dynamical analysis on aromatic compound is very important since they provide the necessary information regarding the chemical reactivity. On the basis of vibrational analysis at HF and B3LYP methods with 6-31+G(d,p) basis set, the standard statistical thermodynamic functions: heat capacity, zero point energy, entropy of TMP have been calculated and are presented in Table 3. The difference in the values calculated by both the methods is only marginal. Scale factors have been recommended for an accurate prediction in determining the zero-point vibration energy (ZPVE), and the entropy (S_{vib}). The variation in the ZPVE seems to be insignificant. Dipole moment reflects the molecular charge distribution and is given as a vector in three dimensions. Therefore, it can be used as descriptor to depict the charge movement across the molecule. Direction of the dipole moment vector in a molecule depends on the centers of positive and negative charges. The total dipole moment of TMP determined by HF and B3LYP methods using 6-31+G(d,p) basis set are 1.4544 and 1.414 Debye, respectively. The total energy and the change in the total entropy of the compound at room temperature are also presented.

CONCLUSION

The optimized geometries, harmonic vibrational wavenumbers and intensities of vibrational bands of TMP have been carried out using the HF and B3LYP methods with the standard 6-31+G(d,p) basis set calculations. The theoretical results were compared with the experimental vibrations, which yield good agreement with the calculated values. From the optimized geometry analysis, we identified that B3LYP/6-31+G(d,p) level of calculation is closer to experimental findings when compared to HF/6-31+G(d,p) of calculation. The TED calculation regarding the normal modes of vibration provides a strong support for the frequency assignment. The calculated first order hyperpolarizability was found to be 2.806×10^{-30} esu, which is 7.5 times greater than reported in literature for urea. The HOMO and LUMO energy gap shows that charge transfer occur within the molecule, which are responsible for the bioactive property of the molecule. The MEP map shows the negative potential sites are on oxygen atom as well as the positive potential sites are around the hydrogen atoms. Furthermore, the thermodynamic and Mulliken charge analysis of the compound have been calculated in order to get insight into the compound.

REFERENCES

1. Sundaraganesan N, Anand B, Meganathan C, Dominic Joshua B, FT-IR, FT-Raman spectra and ab initio HF, DFT vibrational analysis of 2,3-difluoro phenol, Spectrochim. Acta, 68A, 2007, 561-566.
2. Evans JC, The vibrational spectra of phenol and phenol-OD, Spectrochim. Acta, 16A, 1960, 1382-1392.
3. Jayanthi N, Cruz J, Pandiyan T, DFT studies on the phenol and thiophenol interaction on an undecagold cluster surface, Chem. Phys. Lett., 455, 2008, 64–71.
4. Huang J, Huang K, Liu S, Luo Q, Tzeng W, Vibrational spectra and theoretical calculations of *p*-chlorophenol in the electronically excited S_1 and ionic ground D_0 states, J. Photochem. Photobiol. Chem., 193A, 2008, 245-253.
5. Wang G, Gong X, Liu Y, Xiao H, A theoretical study on the vibrational spectra and thermodynamic properties for the nitro derivatives of phenols, Spectrochim. Acta, 74A, 2009, 569-574.
6. Mahadevan D, Periandy S, Ramalingam S, Vibrational spectroscopy (FTIR and FTRaman) investigation using ab initio (HF) and DFT (B3LYP) calculations on the structure of 3-Bromo phenol, Spectrochim. Acta, 78A, 2011, 575-581.
7. Albayrak Ç, Frank R, Spectroscopic, molecular structure characterizations and quantum chemical computational studies of (*E*)-5-(diethylamino)-2-[(2-fluorophenylimino)methyl] phenol, J. Mol. Struct. 984, 2010, 214–220.
8. Koşar B, Albayrak Ç, Cüneyt Ersanlı C, Odabaşoğlu M, Büyükgüngör O, Molecular structure, spectroscopic investigations, second-order nonlinear optical properties and intramolecular proton transfer of (*E*)-5-(diethylamino)-2-[(4-propylphenylimino)methyl]phenol: A

combined experimental and theoretical study, Spectrochim. Acta, 93A, 2012, 1– 9.

9. Demircioğlu Z, Albayrak Ç, Büyükgüngör O, Experimental (X-ray, FT-IR and UV–vis spectra) and theoretical methods (DFT study) of (E)-3-methoxy-2-[(p-tolylimino)methyl]phenol, Spectrochim. Acta, 128A, 2014, 748–758.
10. Yurdakul Ş, Badoğlu S, An FT-IR and DFT study of the free and solvated 4-(imidazol-1-yl) phenol, Spectrochim. Acta, 150A, 2015, 614–622.
11. Frisch MJ, Trucks GW, Schlegel HB, Scuseria GE, Robb MA, Cheeseman JR, Scalmani G, Barone V, Mennucci B, Petersson GA, Nakatsuji H, Caricato M, Li X, Hratchian HP, Izmaylov AF, Bloino J, Zheng G, Sonnenberg JL, Hada M, Ehara M, Toyota K, Fukuda R, Hasegawa J, Ishida M, Nakajima T, Honda Y, Kitao O, Nakai H, Vreven T, Montgomery JA, Peralta JE, Ogliaro F, Bearpark M, Heyd JJ, Brothers E, Kudin KN, Staroverov VN, Kobayashi R, Normand J, Raghavachari K, Rendell A, Burant JC, Iyengar SS, Tomasi J, Cossi M, Rega N, Millam JM, Klene M, Knox JE, Cross JB, Bakken V, Adamo C, Jaramillo J, Gomperts R, Stratmann RE, Yazyev O, Austin AJ, Cammi R, Pomelli C, Ochterski JW, Martin RL, Morokuma K, Zakrzewski VG, Voth GA, Salvador P, Dannenberg JJ, Dapprich S, Daniels AD, Farkas O, Foresman JB, Ortiz JV, Cioslowski J, Fox DJ, GAUSSIAN 09, Revision A.02, Gaussian Inc, Wallingford CT, 2009.
12. Becke AD, Density-functional thermochemistry. III. The role of exact exchange, J. Chem. Phys. 98, 1993, 5648-5652.
13. Lee C, Yang W, Parr RG, Development of the Colle-Salvetti correlation-energy formula into a functional of the electron density, Phys. Rev. B37, 1988, 785-789.
14. Rauhut G, Pulay P, Transferable Scaling Factors for Density Functional Derived Vibrational Force Fields, J. Phys. Chem. 99, 1995, 3093-3100.
15. Sundius T, Scaling of ab initio force fields by MOLVIB, Vib. Spectrosc. 29, 2002, 89-95.
16. MOLVIB (V.7.0): Calculation of Harmonic Force Fields and Vibrational Modes of Molecules, QCPE Program No. 807, 2002.
17. Frisch A, Nielson AB, Holder AJ, Gaussview user manual, Gaussian Inc., Pittsburgh, PA, 2009.
18. Yadav BS, Ali I, Kumar P, Yadav P, FTIR and laser Raman spectra of 2-hydroxy-5-methyl-3-nitropyridine, Indian J. Pure Appl. Phys. 45, 2007, 979-983.
19. Subramanian N, Sundaraganesan N, Jayabharathi J, Molecular structure, spectroscopic (FT-IR, FT-Raman, NMR, UV) studies and first-order molecular hyperpolarizabilities of 1,2-bis(3-methoxy-4-hydroxybenzylidene)hydrazine by density functional method, Spectrochim. Acta, 76A, 2010, 259-269.
20. Sangeetha M, Mathammal R, Mekala R, Crystal Growth and Characterization of p-Arsanilic Acid for Pharmaceutical Application with Theoretical Conformational Study, Int. J. Pharm. Sci. Rev. Res. 34(1), 2015, 47-54.
21. Monicka JC, James C, FT-Raman and FTIR spectra, DFT investigation of the structure and vibrational assignment of mefenacet, J. Mol. Struct., 1095, 2015, 1-7.
22. Arjunan V, Mohan S, Fourier transform infrared and FT-Raman spectra, assignment, *ab initio*, DFT and normal co-ordinate analysis of 2-chloro-4-methylaniline and 2-chloro-6-methylaniline, Spectrochim. Acta, 72A, 2009, 436-444.
23. Socrates G, Infrared and Raman Characteristic Group Frequencies – Tables and Charts, third ed., Wiley, Chichester, 2001.
24. Jeyavijayan S, Arivazhagan M, Study of density functional theory and vibrational spectra of hypoxanthine, Indian J. Pure Appl. Phys. 48, 2010, 869-874.
25. Sajan D, Joe IH, Jayakumar VS, Zaleski J, Structural and electronic contributions to hyperpolarizability in methyl p-hydroxy benzoate, J. Mol. Struct. 785, 2006, 43-53.
26. Powel CE, Humphrey MG, Nonlinear optical properties of transition metal acetylides and their derivatives, Coord. Chem. Rev. 248, 2004, 725-756.
27. Thanthiriwatte KS, de Silva KMN, Non-Linear Optical Properties of Novel Fluorenyl Derivatives-Ab Initio Quantum Chemical Calculations, J. Mol. Struct. (Theochem.) 617, 2002, 169-175.
28. Sun YX, Hao QL, Wei WX, Yu ZX, Lu LD, Wang X, Wang YS, Experimental and density functional studies on 4-(3,4-dihydroxybenzylideneamino)antipyrine, and 4-(2,3,4-trihydroxybenzylideneamino)antipyrine, J. Mol. Struct. (Theochem.) 904, 2009, 74-82.
29. Fleming I, Frontier Orbitals and Organic Chemical Reactions, Wiley, London, 1976.
30. Mulliken RS, Electronic Population Analysis on LCAO-MO Molecular Wave Functions, J. Chem. Phys. 23, 1955, 1833-1840.
31. Murray JS, Sen K, Molecular Electrostatic Potentials, Concepts and Applications, Elsevier, Amsterdam, 1996, pp. 7–624.
32. Scrocco E, Tomasi J, Electronic Molecular Structure, Reactivity and Intermolecular Forces: An Euristic Interpretation by Means of Electrostatic Molecular Potentials, Adv. Quantum Chem. 11, 1978, 115–121.

Source of Support: Nil, **Conflict of Interest:** None.